JOURNAL OF MATERIALS SCIENCE 31 (1996) 3715–3721

Phases in as-spun and aged binary aluminium–lithium ribbons

M. HAJJAJI
Laboratoire de Chimie-Physique, Département de Chimie, Faculté des Sciences Semlalia, B.P. S15, Marrakech, Maroc

L. CUTLER, G. L'ESPERANCE
(CM)², Ecole Polytechnique de Montréal, Box 6079, Succ. A., Montréal, Canada H3C 3A7

As-spun aluminium–lithium ribbons, containing up to 10 wt% Li, and an Al–1.79 wt% Li ribbon aged at different temperatures (room temperature, 66, 175 and 200 °C) were investigated by transmission electron microscopy (TEM) and microhardness testing. It was found that the metastable phase Al_3Li (δ') did not form either in the as-cast ribbons containing less than 1.79 wt% Li or in the featureless zone of Li-rich ribbons (Li content >3 wt%) but it did form, as the stable phase AlLi (δ), in the segregated zone of the later ribbons. The study of the early stage of precipitation showed that the mechanism of formation of δ' depended on the ageing temperature. At a low temperature (66 °C), the δ' phase occurred by homogeneous spinodal decomposition. Whereas, it formed by heterogeneous nucleation at higher temperatures (175 and 200 °C). These results are consistent with the presence of a spinodal curve within the miscibility gap ($\alpha + \delta'$). All investigations performed both on the as-cast and aged ribbons did not reveal any evidence for the formation of G.P. zones. It was also observed in this study that contamination of aluminium–lithium ribbons by impurities such as O_2 and CO_2 could alter the precipitation process and lead to the formation of lithium carbonate.

1. Introduction

The precipitation process in conventionally synthesized aluminium–lithium alloys has been the subject of many studies [1–3], most of which have dealt with the mechanism of formation or the coarsening kinetics of the metastable phase δ' (Al_3Li).

The δ' phase occurs instantaneously upon the quench from solutionizing temperatures. Hence, the initial stages of its occurrence are not well understood and hence its mechanism of formation is still a subject of debate. Nevertheless, two mechanisms have often been reported: (i) the δ' phase forms from the Guinier-Preston (G.P.) zones which develop from Li-saturated solid solution [4–7] and (ii) the δ' phase occurs by spinodal decomposition of the ordered α-solid solution [8–11].

On the other hand, the miscibility gap ($\alpha + \delta'$) locus for the binary Al–Li phase diagram is not completely depicted because of the difficulty in preparing precipitate free aluminium–lithium specimens containing Li over the solubility limit which is in the range 3.7–4.7 wt % [12, 13]. To overcome this difficulty it has been suggested to synthesize specimens by rapid solidification [3], which is known as an efficient technique to extend solid solubility [14].

The first objective of this work is to follow the phase formation in as-rapidly solidified aluminium–lithium ribbons as a function of Li additions. The second objective is to study the mechanism of δ' precipitation in aged aluminium–lithium ribbons.

2. Experimental procedures

Rapidly solidified ribbons of binary aluminium–lithium alloys, containing up to 10 wt % Li (30.2 at %), were prepared from pure metals (Al (99.999%); Li (99.9%)) by the melt spinning technique [15]. The casting process was carried out under a protective He atmosphere, using a casting wheel velocity of 12.5 m s^{-1}.

Amongst the as-cast ribbons, an Al–1.79 wt % Li ribbon free of δ' precipitates (of $\sim$ 60 μm thickness) was chosen for the study of the kinetics of precipitation of the δ' which was conducted at 66, 175 and 200 °C. The ageing procedure was carried out under a dynamic pure argon atmosphere.

For optical metallography and microhardness tests, pieces of ribbon were placed on their longitudinal sections and wrapped in cold setting epoxy. Then, they were conventionally polished and etched by Keller's reagent. The optimum weight used for Vickers microhardness, H_v, experiments was 15 g.

Some ribbons were analysed using a 910 differential scanning calorimeter (DSC) (DuPont Instruments) operating under an inert gas atmosphere. The heating rate used was 10 °C min^{-1}.

0022–2461

The ribbons were also examined by transmission electron microscopy (TEM) using a Jeol 2000 FX apparatus, operating at 200 kV. The thin foils were electropolished by a double-jet of a cold solution (− 10 °C) of perchloric acid and acetic acid (in the molar ratio rate of 1:2) and applying a voltage of 20 V.

3. Results and discussion

3.1. The effect of Li additions on the formation of phases in the as-spun ribbons

In the first step of this study, the microhardness of as-cast Al–Li ribbons was measured as a function of Li concentration. As shown in Fig. 1, H_v increases moderately up to around 2 wt % Li. Whereas, it exhibited a marked increase in the composition range 2–3 wt % Li. Accordingly, two distinct hardening behaviours may be discerned.

In order to understand the origin of the first hardening, H_v was plotted as a function of the square root of Li composition (in at %). The linear relationship observed from 0 to around 7 at % Li (Fig. 2) characterizes a solid solution hardening [16]. Indeed, X-ray diffraction (XRD) and TEM analyses showed that α solid solution was the only phase found in ribbons containing less than 1.79 wt % Li (6.64 at %). A typical TEM micrograph and its associated selected area diffraction (SAD) pattern are shown in Fig. 3.

The second important strengthening is attributed to the simultaneous formation of δ and δ′ phases in Li-rich ribbons (wt % Li > 3). The abundant and dispersed particles of the metastable phase δ′ (Fig. 4a) were observed especially in the segregated zone which constituted around the top two-thirds of the ribbon thickness. Their size (around 6 nm in diameter) was less affected by Li content. Whereas, only a few particles of the δ phase, as seen in Fig. 4b, were formed, mainly in the area neighbouring the ribbon free surface and they became coarser with Li additions. Meanwhile, the microhardness experienced a slight decrease.

It was observed that all the as-rapidly solidified ribbons enclosed a high density of dislocations.

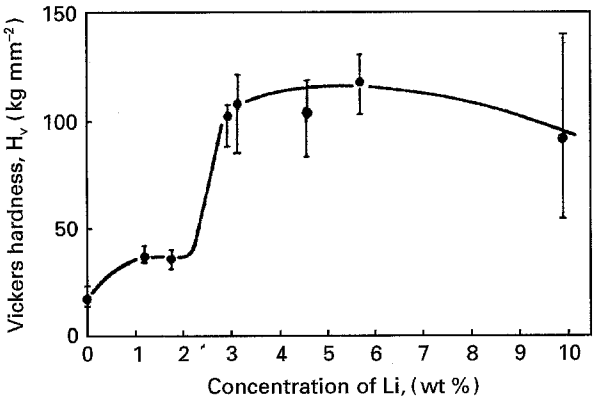

Figure 1 Effect of Li additions on the microhardness of as-cast aluminium–lithium ribbons.

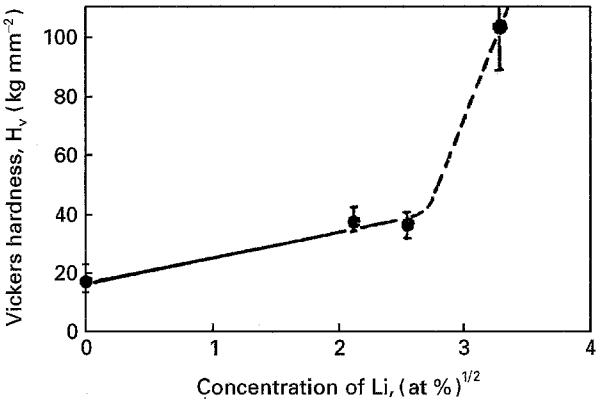

Figure 2 Microhardness of rapidly solidified ribbons as a function of the square of Li content (in at %).

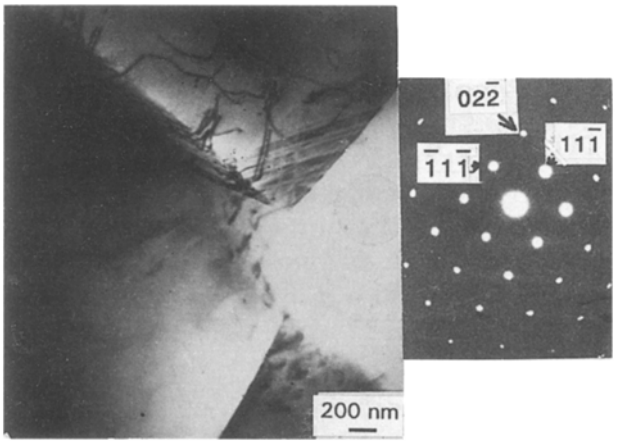

Figure 3 TEM micrograph of as-spun Al–1.79 wt % Li ribbon (mid thickness region) and its associated SAD pattern (zone axis: $[0\,1\,1]_\alpha$).

It is observed that the δ′ and δ phases did not occur in the supersaturated solid solution (labelled featureless zone), located near the cooled side of the Li-rich ribbons [17], it may be stated that these phases, which developed only in the segregated zone, nucleated from the melt. This is due to the segregation of Li due to the reduction of the growth rate in the vicinity of the cooled ribbon surface. Moreover, because of the relatively low velocity (12.5 m s^{-1}) of the casting wheel, it is expected that the contact time between the heat sink and ribbon would be high. Consequently, before the ribbon left the wheel surface its temperature dropped drastically. Under such a condition, precipitation in the supersaturated solid solution would be hindered and the size of the δ′ precipitates could not evolve.

3.2. Precipitation in aged ribbons

3.2.1. Ageing at room temperature

According to the results of Papazian *et al.* [5], the G.P. zones must develop at low temperatures in aluminium–lithium alloys containing small amounts of Li and disappear upon heating in the temperature range 100–150 °C. To investigate the formation of these precursors, at very low temperature, the Al–1.79 wt % Li ribbon was aged for 9 months at room temperature,

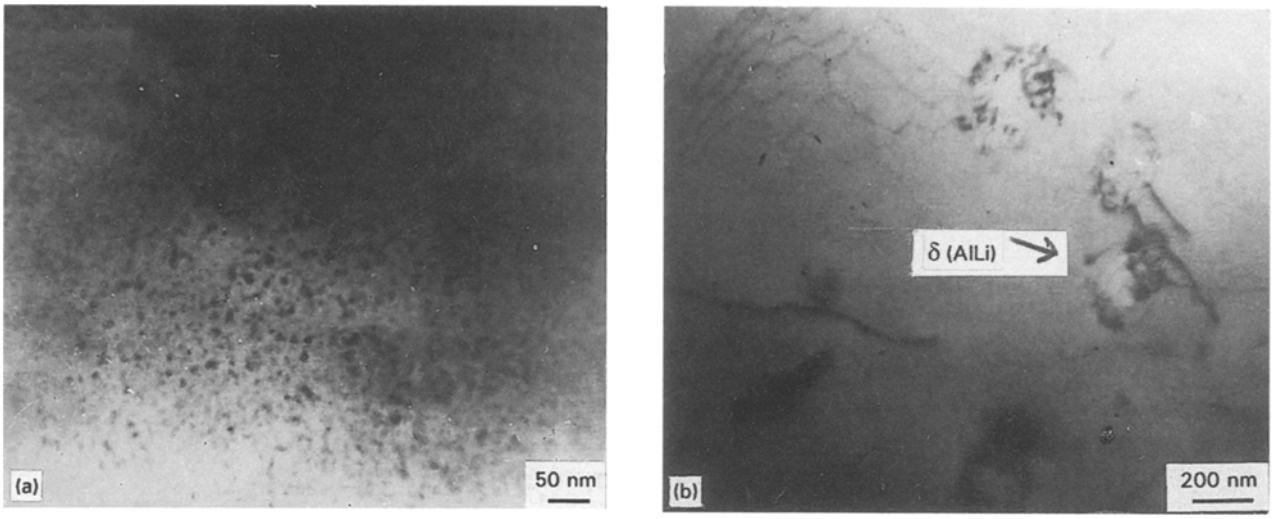

Figure 4 Microstructure of rapidly solidified Al–3.14 wt % Li ribbon (a) δ′ phase in the mid thickness zone (g = 110 zone axis: [0 0 1]); (b) δ phase in the unchilled side (g = 110; zone axis: [1 $\bar{1}$ 1]).

under a rarefied atmosphere (around 570 mm Hg); then, analysed by DSC. As seen in Fig. 5, the heat flow curve exhibited a smooth evolution that indicates the absence of precipitation and dissolution reactions. Furthermore, the microstructure of the aged and as-cast ribbons, examined by TEM, displayed the same features.

Owing to the small dimensions of the ribbon (surface/volume $\approx$ 1), the great chemical affinity of Li for moisture in the air and the facile Li-diffusion in this rapidly solidified ribbon (as reported in the next paragraph) it seems that an important quantity of Li was lost from the bulk of the specimen leading to the formation of a Li-poor solid solution thus preventing the eventual occurrence of G.P. zones or the precipitation of Li-rich phases.

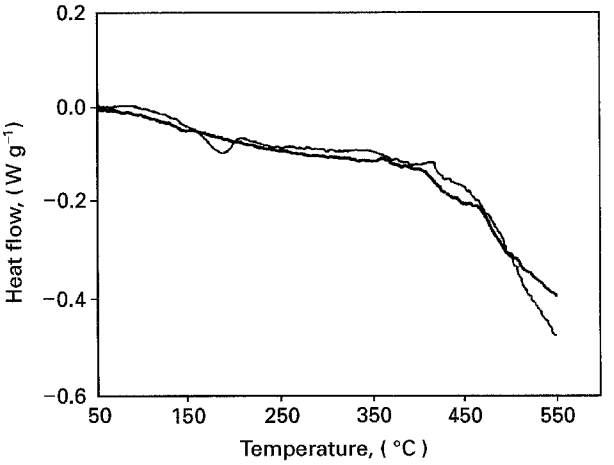

Figure 5 DSC thermogram of Al–1.79 wt % Li ribbon aged at (—) 9 months at room temperature and (—) 6 months at 66 °C.

3.2.2. Ageing at 66 °C

The theoretical Al–Li phase-diagram reported by Sigli *et al.* [18] predicts at low temperatures (< 100 °C) the formation of G.P. zones in the composition range 1–16 at % Li. If the Al–6.64 at % Li ribbon is aged at 66 °C it will decompose into α solid solution and G.P. zones. The occurrence of such Li-rich zones would produce a strengthening which may be revealed by a microhardness test.

The age hardening curve of Al–6.64 at % Li ribbon (Fig. 6) showed a monotonous increase and, as can be seen, the onset of hardening could not be accurately determined. However, it has been observed from the depiction of $H_v = f(t^{1/2})$ (where t is the ageing time) that the hardening phenomenon started at around 10 days of ageing.

TEM examinations conducted on specimens aged up to 117 days exhibited only the precipitate free α solid solution. A typical micrograph and its associated SAD pattern are shown in Fig. 7. After 6 months of ageing, very fine δ′ precipitates (around 3.7 nm in diameter), were homogeneously formed throughout the matrix and were not affected by the presence of dislocations or grain boundaries (Fig. 8).

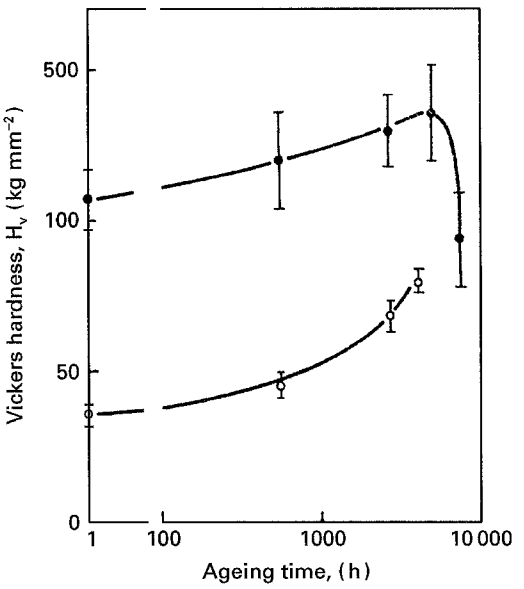

Figure 6 Age hardening curves (T = 339 K) at (○) Al–1.79 wt % Li: and (●) Al–3.14 wt % Li.

Since there is no evidence for the formation of G.P. zones and the ordered domains of δ′ were not affected by the structural defects, it seems that the δ′ was

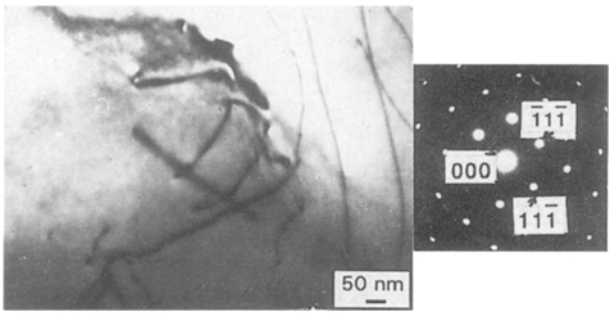

Figure 7 Free precipitate α solid solution in Al–1.79 wt % Li, aged 23 days at 66 °C (zone axis: $[0\,1\,1]_\alpha$).

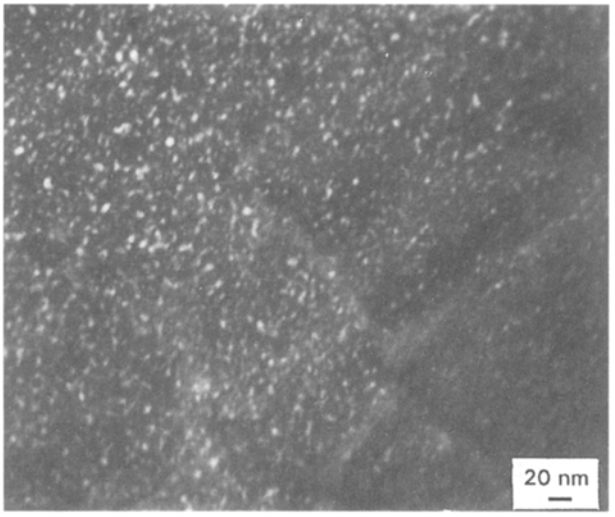

Figure 8 Homogeneous precipitation of δ′ in Al–1.79 wt % Li ribbon aged 6 months at 66 °C (g = $\bar{1}\,0\,0$; zone axis: [0 1 1]).

produced at this temperature by spinodal decomposition as suggested by Miyasato and Thomas [19]. The formation of δ′ required at least 10 days. Presumably, over such a time period the disordered solid solution of the as-cast ribbons transformed into an ordered solid solution which was in turn decomposed to the α and δ′ phases.

The aged specimen, containing δ′ phase, was analysed using the differential scanning calorimetry technique. The thermogram, shown in Fig. 5b, displayed an endothermic peak at 108.4 °C which is attributed to the dissolution of the δ′ phase. The heat involved in this process is around 14.5 $J\,g^{-1}$.

Based on the linear relationship between the heat of dissolution and the volume fraction of δ′ [20], the δ′ weight fraction ($f_{\delta'}$) was estimated to be 8.4% and the concentration of solute in the matrix (C_α) in equilibrium with the δ′ precipitates was then determined from the lever rule expression:

$$f_{\delta'} = \frac{C_0 - C_\alpha}{C_{\delta'} - C_\alpha}$$

where, C_0 is the initial Li composition (1.79 wt %) and $C_{\delta'}$ is the Li content with the δ′ precipitates (7.9 wt %). The calculated value 1.23 wt % Li (4.6 at %) of C_α is very close to that deduced from the metastable solvus curve (5 at %) published by Williams [3].

According to the studies performed on the δ′ coarsening kinetics [1–3], the average radius ($\bar{R}$) of δ′ at a time t obeys the equation:

$$\bar{R}^3 - \bar{R}_0^3 = kt \qquad (1)$$

where $\bar{R}_0$ is the initial particle size and k is the rate constant which depends on the solute diffusion coefficient (D) as follows:

$$k = \frac{8}{9}\frac{\gamma\, C_e D\, V_m^2}{RT}$$

here, γ is the surface tension ($\gamma = 0.014\ J\,m^{-2}$ [21]); V_m is the molar volume of δ′ ($V_m = 10^{-5}\ m^3\,mol^{-1}$) and the product RT has the usual meaning. C_e ($mol\,m^{-3}$) is the Li concentration of the matrix in equilibrium with the δ′ precipitates.

C_0 and C_e (in wt % Li) are related through the equation:

$$C_e = \frac{C_\alpha \rho}{M_{Li}}$$

with ρ the alloy density ($\rho = 2.7 \times 10^{-3} - 76.9 \times 10^{-3}$ (wt % Li)) [22] and M_{Li} the molar mass of lithium.

Referring to the previous results, it may be assumed that $\bar{R}_0$ is zero up to 10 days of ageing. Therefore, Equation (1) is reduced to

$$\bar{R}^3 = kt \qquad (2)$$

The mean value of $\bar{R}$, determined from the particle size distribution diagram (Fig. 9a), allows us to calculate the Li diffusion coefficient at 66 °C which was found to be around $2.2 \times 10^{-22}\ m^2\,s^{-1}$. This value is about 1000 times higher than the calculated one using the Costas expression [23]:

$$D = 4.5 \times 10^{-4} \exp(-139.2/8.31 \times 10^{-3} T)\ m^2\,s^{-1}$$

which was established in the case of a conventionally synthesized Al–Li alloy. This large difference is likely due to the higher concentration of crystalline defects formed in the rapidly solidified alloys.

3.2.3. Ageing at 175 and 200 °C

The hardening curves of an Al–1.79 wt % Li ribbon aged at 175 and 200 °C (Fig. 10) had a roughly similar trend, that is, they exhibited a plateau in the first stage of ageing and a very pronounced peak for long ageing times.

TEM examinations of several aged specimens showed that the microstructure did not experience an appreciable change during the first few minutes of ageing. At the end of 20 min of ageing at 175 °C only very fine and heterogeneous precipitates of δ′ which were difficult to image, were detected. Similar δ′ precipitates with a more developed size were also observed in the specimen aged 40 min at 200 °C (Fig. 11). These precipitates occurred heterogeneously as agglomerates and coalesced mainly along dislocations to form plates (Fig. 12). This type of coalescence was also reported by Baumann and Williams [24] who attributed the change of the δ′ morphology to the fact that the solute supply is radially important but relatively limited along dislocations.

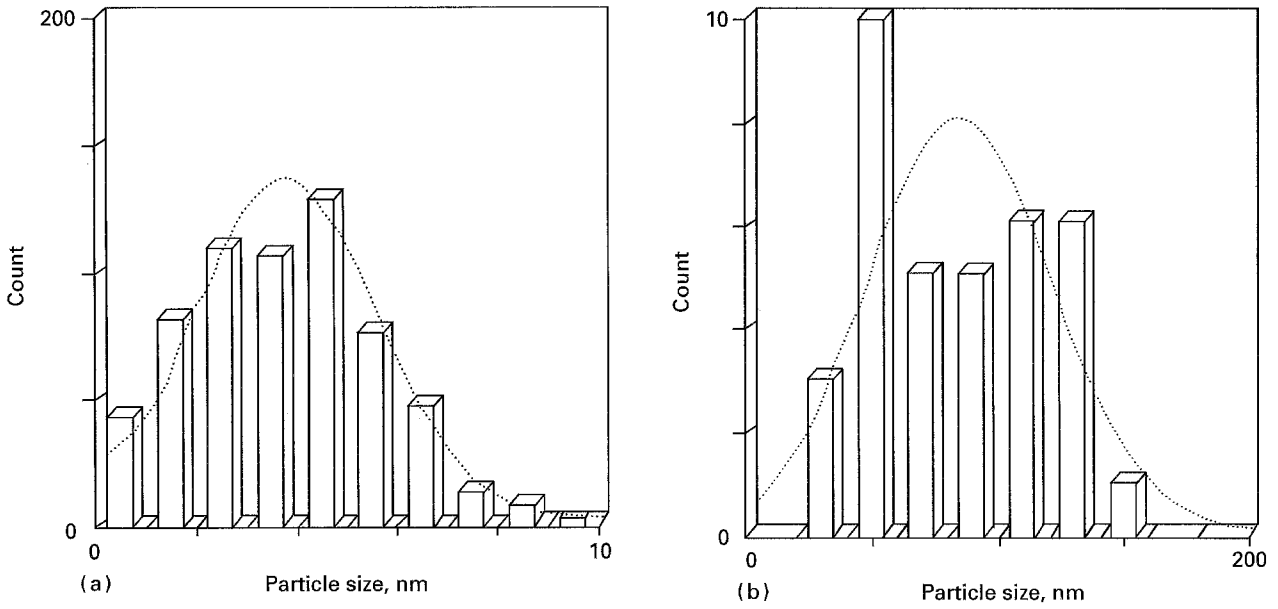

Figure 9 Particle–size distribution histogram of δ′ in Al–1.79 wt % Li ribbon aged at: (a) 66 °C for 171 days; (b) 200 °C for 8.2 days.

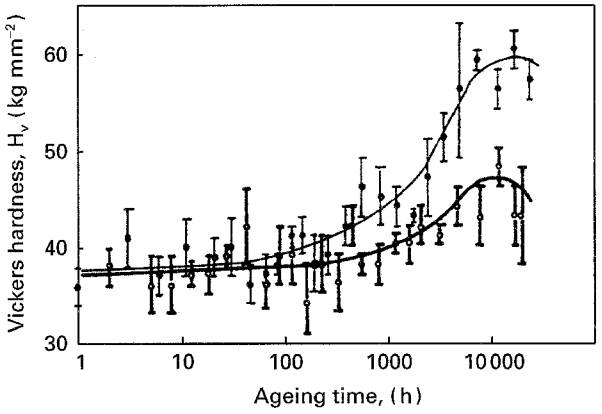

Figure 10 Age hardening curves of Al–1.79 wt % Li ribbon at (●) T = 448 K and (○) T = 473 K.

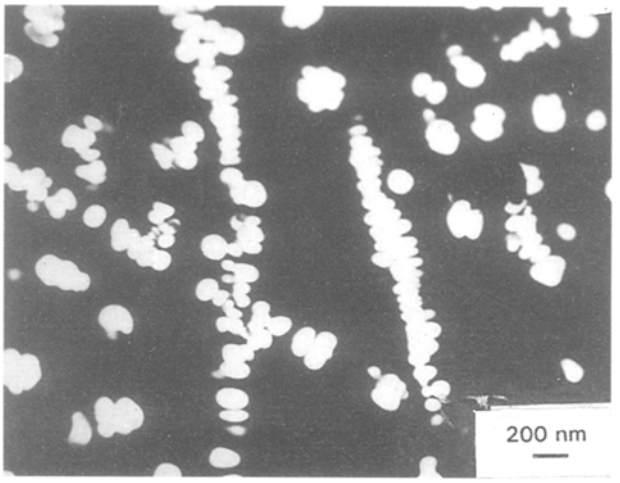

Figure 12 Coarsened δ′ precipitates in Al–1.79 wt % Li ribbon aged 17.3 days at 175 °C (g = 110; zone axis: [$\bar{1}$ 1 4]).

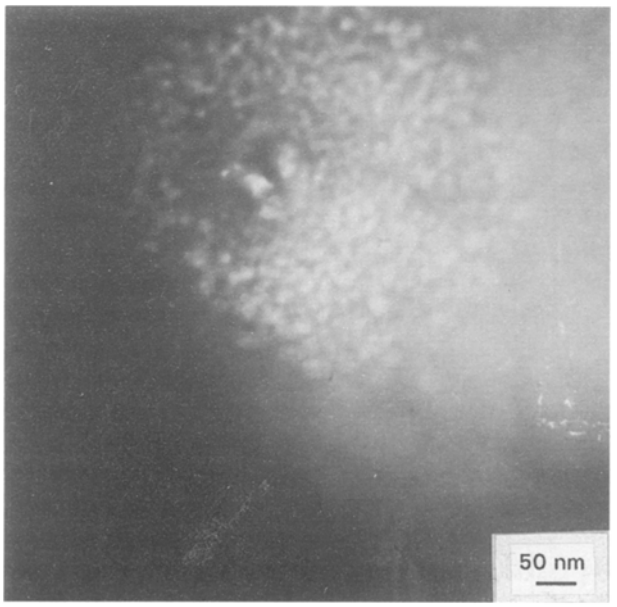

Figure 11 Heterogeneous precipitation of δ′ in Al–1.79 wt % Li aged 40 min at 200 °C (g = $\bar{2}\,\bar{1}\,0$; zone axis: [$\bar{1}$ 2 3]).

Considering the mean diameter of δ′ precipitates, determined from the histogram depicted in Fig. 9b, and the growth, Equation (2) ($\bar{R}_0$ is assumed to be zero for $t \leqslant 4$ min), the calculated rate constant at 200 °C is around 90×10^{-3} nm^3 s^{-1}. Using the Arrhenius equation, the calculated activation energy for δ′ coarsening in these binary Al–Li alloys is 121 kJ mol^{-1}. This value is very close to those given in the literature [25–27].

From this precipitation kinetic study it is emphasized that the G.P. zones did not form at these temperatures and the hardening process is only due to the δ′ phase which occurred heterogeneously by nucleation from the saturated α solid solution.

3.3. Effect of contaminants on the stability of δ′ and δ phases

The as-cast Al–3.14 wt % Li ribbon, containing δ and δ′ phases in the segregated zone, was aged at 66 °C under a dynamic pure argon atmosphere.

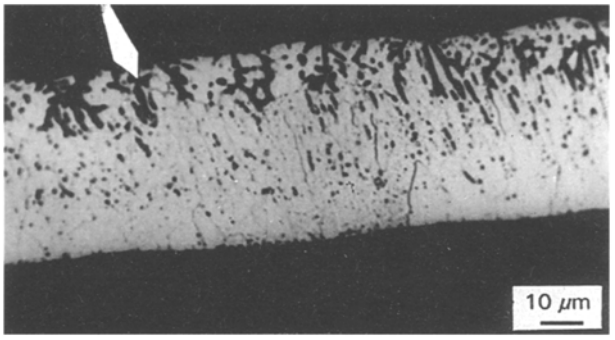

Figure 13 Longitudinal section of Al–3.14 wt % Li ribbon aged at 66 °C for 220 days (chilled side at bottom).

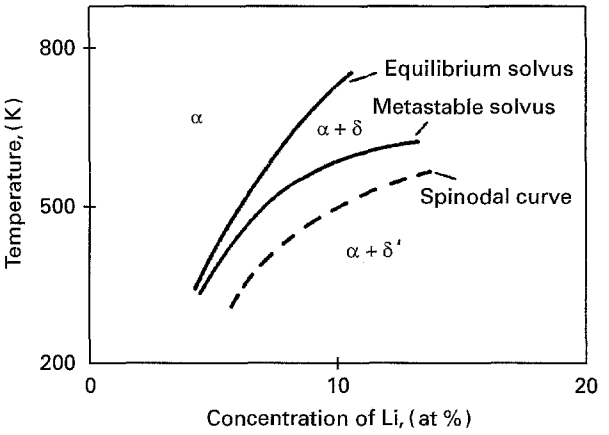

Figure 14 Al-rich domain of Al–Li phase diagram.

TEM examinations carried out on thin foils prepared especially from the featureless zone (the bottom-third of the thickness) of several aged specimens exhibited, after 117 days of ageing, a homogeneous precipitation of δ′, similar to that seen in Fig. 8. Meanwhile, the microhardness increased, but, it drastically dropped after around 220 days of ageing (Fig. 6).

Metallographic examinations performed on longitudinal sections of the ribbon aged for 220 days revealed a beginning of the disappearance of the columnar structure (as pointed out by the arrow in Fig. 13) and the X-ray diffraction analysis showed the presence of Li_2CO_3 as a contaminant. However, when the ageing time reached 323 days, all the X-ray peaks assigned to the δ′ and δ precipitates vanished and the carbonate was the dominant phase. Further examinations particularly performed by TEM confirmed this result since only α solid solution grains were present in addition to the Li_2CO_3.

Because of the great chemical affinity of Li to atmospheric impurities [28], the Li-rich phases (AlLi and Al_3Li) reacted with the oxygen and the carbon dioxide of the atmosphere which led to the formation of carbonate probably by the mechanism reported by Field and Butler [29].

4. Conclusion

Rapid solidification of binary aluminium–lithium alloys by the melt spinning technique impeded the formation of δ′ and δ phases in ribbons containing less than 1.79 wt % Li and in the featureless zone which was formed in the chilled side of Li-rich ribbons (wt % Li > 3). However, it favoured the formation of these phases in the segregated zone.

It is emphasized from results of this study that there was no evidence to support the formation of G.P. zones in the as-cast and aged aluminium–lithium ribbons.

The precipitation of the δ′ phase evolved by one of the following mechanisms: at low temperature (66 °C) δ′ occurred by homogeneous spinodal decomposition. For higher temperatures (175 and 200 °C) it, however, nucleated heterogeneously and preferentially grew on dislocations. These results are consistent with the presence of a spinodal curve as proposed qualitatively in the phase diagram depicted in Fig. 14.

The contamination of Al–Li alloys by oxygen and carbon dioxide of the protective atmosphere prevented the development of δ′ and δ phases since the Li is tied up in Li_2CO_3.

References

1. D. B. WILLIAMS, in "Aluminium–lithium I", edited by T. H. Sanders Jr. and E. A. Starke Jr., (TMS-AIME, Warrendale, PA, 1981), p. 89.
2. T. H. SANDERS Jr, and E. A. STARKE Jr. "Aluminium–lithium II", (TMS-AIME, Warrendale, PA, 1984), p. 1.
3. D. B. WILLIAMS, in "Aluminium–lithium V", edited by T. H. Sanders Jr. and E. A. Starke Jr. (Materials and Component Engineering Publications Ltd. (MCEP), Birmingham, U.K. 1989), p. 551.
4. R. NOZATO and G. NAKAI, *Trans. Jpn. Inst. Metals.* **18** (1977), p. 679.
5. J. M. PAPAZIAN, C. SIGLI and J. M. SANCHEZ, *Scripta Metall.* **20** (1986) 201.
6. A. K. MUKHOPADHYAN, C. N. J. TITE, H. M. FLOWER, P. J. GREGSON and F. J. SALE, in "Aluminium–lithium IV" edited by G. Champier, B. Dubost, D. Mianny and L. Saletay (Les Editions de Physique, Paris, 1987), p. 439.
7. A. LIVET, D. BLOCH, *Scripta Metall.* **10** (1985) 1147.
8. T. SATO, A. TANAKA and T. TAKAHASHI, *Trans. Jpn. Inst. Metals.* **29** (1988) 17.
9. V. RADMILOVIC, A. G. FOX and G. THOMAS, *Acta Metall. Mater.* **37** (1989) 2385.
10. S. FUJIKAWA, M. FURUSAKA, M. SAKAUCHI and K. HIRANO, *J. de Phys. Coll. C3*, **48** (1987) 365.
11. A. G. KHACHATURYAN, T. F. LINDSEY and J. W. MORRIS Jr, *Metall. Trans. A* **19A** (1988) 249.
12. A. J. MCALISTER, Bull. Alloy Phase Diagrams, Vol. 3, (1982), p. 177.
13. C. CHEN SINN-WEN, Y. AUSTIN and G. CHU MEN, Aluminium–lithium V, edited by T. H. Sanders Jr. and E. A. Starke Jr., (Materials and Component Engineering Publications Ltd. (MCEP), Birmingham, U.K. 1989), p. 585.
14. H. JONES, *J. Mater. Sci.* **19** (1984) 1043.
15. M. HAJJAJI, Ph.D. thesis, Ecole Polytechnique de Montréal (Canada), 1990
16. M. VAN ROOYEN, P. F. COLIJN, T. H. H. DE KEIJSER and E. J. MITTMEIJER, *J. Mater. Sci.* **21** (1986) 2373.
17. M. HAJJAJI, L. CUTLER and G. L'ESPÉRANCE, *J. Mater. Sci.* **31** (1996) 1027.
18. C. SIGLI and J. M. SANCHEZ, *Acta Metall. Mater.* **34** (1986) 1021.
19. S. MIYASATO and G. THOMAS, in "Aluminium–lithium V", edited by T. H. Sanders Jr. and E. A. Starke Jr. (Materials and Component Engineering Publications Ltd. (MCEP), Birmingham, U.K. 1989), p. 633.

20. J. LENDVAI, H. J. GUDLADT, W. WUNDERLICH and V. GEROLD, *Z. Metallkd*, **80** (1989) 310.
21. S. F. BAUMANN and D. B. WILLIAMS, *Acta Metall. Mater.* **33** (1985) 1069.
22. E. J. LAVERNIA and N. J. GRANT, *J. Mater. Sci.* **22** (1987) 1521.
23. L. P. COSTAS, U.S. Atomic Energy Commission Report (D.P. 813), (1963).
24. S. F. BAUMANN and D. B. WILLIAMS, *Metall. Trans. A* **16A** (1985) 1203.
25. B. NOBLE and G. E. THOMPSON, *Metal. Sci. J.* **5** (1971) 114.
26. P. L. MAKIN and B. RALPH, *J. Mater. Sci.* **19** (1984) 3835.
27. M. K. AYDINOL and A. S. BOR, *ibid.* **29** (1994) 15.
28. M. HAJJAJI, L. CUTLER and G. L'ESPÉRANCE, *J. Alloys and Compounds* **188** (1992) 194.
29. D. J. FIELD and E. P. BUTLER, in "Aluminium–lithium I", edited by T. H. Sanders Jr. and E. A. Starke Jr. (TMS-AIME, Warrendale, PA, 1981), p. 667.

Received 28 June 1995
and accepted 21 December 1995